Laser-annealing-made amplified spontaneous emission of "giant" CdSe/CdS core/shell nanocrystals transferred from bulk-like shell to quantum-confined core

Chen Liao, Kai Fan, Ruilin Xu, Huichao Zhang, Changgui Lu, Yiping Cui, and Jiayu Zhang*

Advanced Photonic Center, Southeast University, Nanjing 210096, China
**Corresponding author: jyzhang@seu.edu.cn*

Received May 28, 2015; revised July 3, 2015; accepted July 4, 2015;
posted July 6, 2015 (Doc. ID 241875); published August 7, 2015

"Giant" CdSe/CdS core/shell nanocrystals (NCs) were synthesized with thick CdS shell (15 monolayers), and the x-ray diffraction (XRD) measurement indicates there is a zinc blende phase in the thick CdS shell, whereas it transformed into wurtzite phase under 5 min radiation with a 400 nm, 594 $\mu J/cm^2$ femtosecond (fs) laser beam. The evolution of the NCs' spontaneous emission under the fs laser radiation was recorded with a Hamamatsu streak camera. The as-synthesized NCs exhibit an amplified spontaneous emission (ASE) at 530 nm, which comes from a bulk-like CdS shell due to the interfacial potential barrier, which could slow down the relaxation of holes from the shell to the core. After being annealed by an fs laser, the ASE of the g-NCs is transferred from a bulk-like CdS shell to a quantum-confined CdSe core because the phase transformation determined with the XRD measurement could remove the interfacial barrier. Besides the ASE at 643 nm, two shorter-wavelength ASE peaks at 589 and 541 nm, corresponding to optical transitions of the second (1P) and third (1D) electron quantization shells of the CdSe core, also appear, thus indicating that Auger recombination is effectively suppressed.

OCIS codes: (140.3390) Laser materials processing; (140.5960) Semiconductor lasers; (160.3380) Laser materials.
http://dx.doi.org/10.1364/PRJ.3.000200

1. INTRODUCTION

Due to the quantum confinement effect, colloidal semiconductor nanocrystals (NCs) exhibit various advantageous properties as optical gain media, including emission wavelength tunability over a wide spectral range through simply changing the size of the NCs, temperature-insensitive lasing performance, and potentially low lasing threshold [1]. However, the development of lasers based on colloidal NCs are hindered by Auger recombination, wherein the energy of one electron–hole pair (exciton) is nonradiatively transferred to another charge carrier [2]. This process severely limits the lifetime and bandwidth of optical gain [1]. Recently, Klimov *et al.* synthesized a new class of NCs (termed "giant" NCs or g-NCs), which comprise a small CdSe core (3–4 nm diameter) encapsulated in a thick shell [>10 monolayers (MLs)] of a wider bandgap CdS [3]. Those g-NCs can reduce the rate of Auger transitions by partially separating electron and hole wave functions due to their quasi-type-II band alignment [4]. As a result, in the g-NCs with an 11 MLs CdS shell, even multiexcitons of a high order (13th and possibly higher) exhibit high emission efficiencies and contribute to optical gain [5]. Further studies show that, in order to better suppress Auger recombination [6,7] and enhance chemical/photostability [3], thicker shells are necessary.

In contrast with moderate-shell (~10 MLs) g-NCs, the ultrathick-shell g-NCs feature an interfacial potential barrier in the valence band associated with a thin zinc blende (ZB) CdS layer separating the ZB CdSe core from the thick wurtzite (WZ) CdS shell, as shown in Fig. 1(c) [8]. Because of this barrier, relaxation of "hot" holes from the shell (which has a much greater absorption cross section than the core [5]) to the core in those NCs is dramatically slowed, to the point at which radiative recombination from high-lying shell-based states becomes competitive [8–10]. As a result, under intense excitation with subpicosecond laser pulses, the NCs exhibit an amplified spontaneous emission (ASE) from a bulk-like CdS shell instead of quantum-confined CdSe core [11,12]. In most cases, this is not what we want. For NCs' lasing application, the ASE from the quantum-confined core is better than that from a bulk-like shell [1].

In this paper, we synthesized CdSe/CdS core/shell g-NCs that comprise a small CdSe core (4 nm diameter) encapsulated in a thick shell (15 MLs) of CdS [Figs. 1(b) and 1(c)] and focus on removing interfacial potential barrier through fs laser annealing and, consequently, transferred ASE of the g-NCs from bulk-like CdS shell to quantum-confined CdSe core. Besides the ASE at 643 nm, two shorter-wavelength ASE peaks corresponding to optical transitions of the second (1P) and the third (1D) electron quantization shells of CdSe core also appear, thus indicating that Auger recombination is effectively suppressed.

2. PREPARATION OF CdSe/CdS g-NCs

We followed conventional procedures to synthesize the NCs [7,13].

The cores of CdSe NCs were synthesized by a general method. The mixture of CdO (0.128 g), oleic acid (OA) (2.26 g), and 1-octadecene (ODE) (30 g) in a three-necked

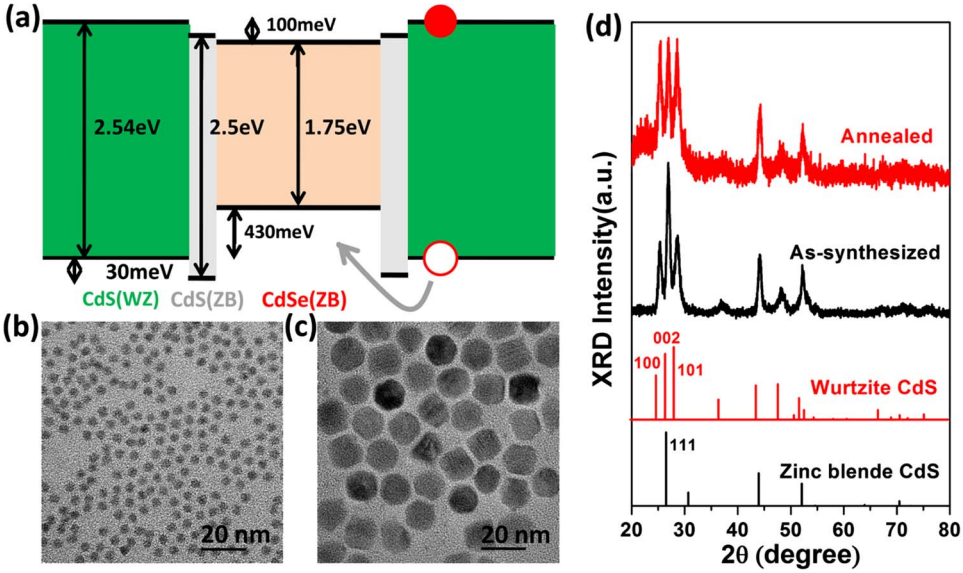

Fig. 1. (a) Band structure of a CdSe/CdS core/shell g-NC features an energetic barrier in the valence band associated with an interfacial ZB CdS layer, which separates a thick WZ CdS outer layer from the ZB CdSe core. (b) Transmission electron microscopy images of CdSe cores and (c) their corresponding CdSe/CdS core/shell (15 MLs) g-NCs. (d) XRD patterns of as-synthesized and annealed CdSe/CdS core/shell (15 MLs) g-NCs. Vertical lines indicate WZ and ZB CdS bulk reflections.

flask (250 mL) was heated to about 240°C to obtain a colorless clear solution. After this solution was cooled to room temperature, octadecylamine (ODA) (7.5 g) and oleylamine (OL) (5 mL) were added into the flask. Under argon flow, this system was reheated to 280°C. At this temperature, a selenium solution (2.5 mL) created by dissolving Se powder (1.9 g) in tributylphosphine (TBP) (8.2 g) was quickly injected. The growth temperature was then reduced to 250°C. When the desired particle size was reached, the reaction mixture was cooled to room temperature, and then CdSe NCs were purified and dissolved in n-hexane to be the CdSe core for the following shell growth.

The CdSe/CdS core/shell g-NCs were prepared with the successive ionic layer adsorption and reaction method [14]. The cadmium precursor solution (0.1 M) was prepared by mixing CdO (0.385 g), OA (6.778 g) with ODE (17.64 g), and a clear solution was obtained at 250°C under Ar flow. The sulfur precursor solution (0.1 mol/L) was prepared by dissolving sulfur (0.096 g) in ODE (23.67 g) at 100°C under Ar flow. The amount of cadmium or sulfur precursors required for each ML was determined by the volume increment of every shell and the NC's particle concentration. The above CdSe NCs were mixed with OL (10 mL) and octadecane (OD) (30 g) in a three-necked flask. After removal of the hexane under vacuum at 60°C, the mixture was heated to 240°C under Ar flow where the 1–5 MLs shell growth was performed. The core/shell CdSe/CdS NCs were formed by alternating addition of the Cd precursor and the S precursor with a period of 10 min. For the 6–15 MLs shell growth, the growth temperature was increased to 280°C, and the period between each addition was extended to 30 min.

3. RESULTS AND DISCUSSION

In our synthesis of core/shell g-NCs, we use presynthesized CdSe seeds with a ZB structure. In agreement with previous observations for CdSe/CdS NCs, the first few MLs of CdS grow epitaxially on top of the CdSe core [thin gray shell in Fig. 1(a)] [8–10,15,16]. X-ray diffraction (XRD) studies show that, for the as-synthesized CdSe/CdS (15 MLs) g-NCs, the outer CdS layer is mainly a WZ phase [Fig. 1(d)]. However, the diffraction peak at 26.9° is evidently strong than that at 25.4° and 28.5°, which is likely due to the contribution of (111) plane of the ZB CdS structure, indicating that there is a thin ZB CdS layer directly adjacent to the CdSe core. The nonuniformity in the shell crystal structure results in an energetic barrier at the core/shell interface [Fig. 1(a)], which could slow down the relaxation of holes from the shell to the core [8–10]. Under 5 min radiation with a 400 nm 594 $\mu J/cm^2$ fs laser beam, the diffraction peak of the annealed g-NCs at 26.9° is dramatically reduced, thus indicating the interfacial barrier is removed. Moreover, the negligible change in the FWHM of the XRD peaks indicates a slight change of the g-NCs' crystallinity after laser annealing.

Figure 2(a) shows that the CdSe cores' first-exciton absorption peak and photoluminescence (PL) peak were located at 594 and 603 nm, respectively. With the deposition of the CdS shell, the first-exciton absorption peak and PL peak of CdSe/CdS core/shell NCs shift to the red due to electron delocalization into the shell region, while the hole remains primarily confined to the core [5]. As a result, the first exciton absorption peak and PL peak of the CdSe/CdS core/shell (15 MLs) g-NCs were shifted to 632 and 646 nm, respectively. The PL redshift is accompanied by a significant increase of the absorption cross section at shorter wavelength because in g-NCs light absorption is primarily due to a much larger CdS shell, which completely overwhelms a much weaker first-exciton absorption feature of the CdSe core. The globe Stokes shift (the spectral separation between PL emission and the principal absorption onset of the NCs) [17] is ~120 nm for the g-NCs with 15 MLs CdS shells. Due to g-NCs' quasi-type-II band alignment, the average lifetime of CdSe/CdS (15 MLs) g-NCs (87 ns) is evidently longer than that of CdSe cores (18 ns) [Fig. 2(b)].

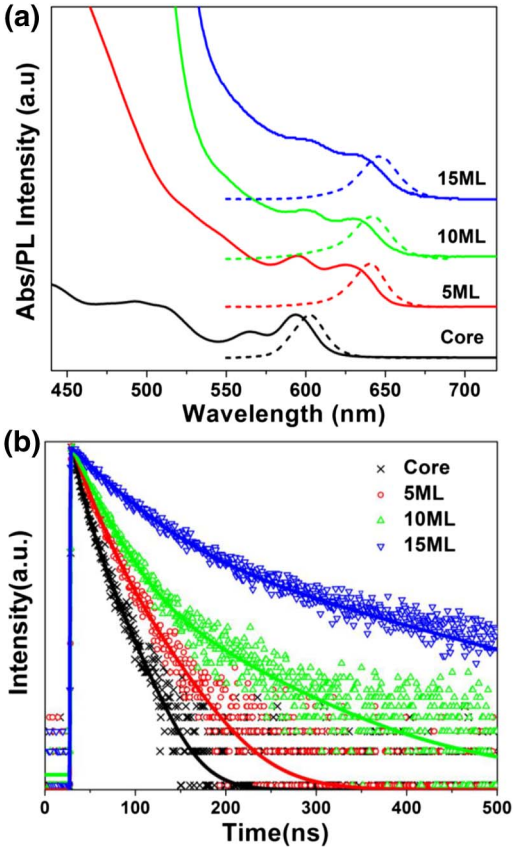

Fig. 2. (a) Absorption (solid line) and PL (dash line) spectra of the CdSe core and its corresponding CdSe/CdS core/shell NCs. (b) Time-resolved PL decay spectra of the CdSe core and its corresponding CdSe/CdS core/shell NCs. The solid lines are the bi-exponential fitting curves.

The time-resolved PL decay spectra of CdSe/CdS core/shell (15 MLs) g-NCs solution under intense excitation [Fig. 3(a)] were measured by a streak camera (Hamamatsu C5680). The light beam was from Ti:sapphire regenerative amplifier (Coherent Legend-F-1k), whose central wavelength, pulse duration, and repetition rate were 800 nm, 100 fs, and 1 kHz, respectively. Excitation pulses at 400 nm were obtained by doubling the fundamental wavelength in a β-barium borate (BBO) crystal. Figures 3(b) and 3(c) show the PL spectra of the g-NCs as a function of time delay with respect to the laser pulse. Immediately after excitation, the PL spectrum contained emission both at 642 and 504 nm. The g-NCs exhibit green emission (504 nm), which comes from bulk-like CdS shell because the hole relaxation from the shell into the core is hindered by the combined effect of Coulombic repulsion of the holes already in the core and an intrinsic potential barrier at the shell/core interface revealed by the XRD studies [Figs. 1(a) and 1(d)] [8–10]. As illustrated in Fig. 3(d), the green emission decayed faster than the experimental resolution. Picosecond time-resolved measurement confirmed that the lifetime of the green emission was 280 ps, which was consistent with that of bulk CdS. The red emission peak (642 nm) was slightly blueshifted with respect to the emission peak (646 nm) measured 11 ns after excitation, which corresponded to single exciton emission, due to exciton–exciton repulsion [5]. The blueshift was slight, and no obvious fast decay component in PL decay spectra measured at 646 nm was observed, thus indicating the ratio of g-NCs, which contain two excitons, is small.

The ASE of CdSe/CdS core/shell (15 MLs) g-NCs were studied in pulsed stripe photoexcitation experiments (Fig. 4). Pump stripe length and width are 4 mm and 40 μm, respectively, and the emission is collected from the edge of the film. For as-synthesized g-NCs, at low excitation fluences, we observe spontaneous emission (SPE) at 652 nm. As the fluence increases, a peak develops on the short wavelength side (530 nm) of the SPE band [Fig. 4(a)], which is together with a superlinear dependence on pump fluence [Fig. 4(b)], thus indicating the ASE process, while the growth of the 652 nm SPE peak is sublinear. In agreement with previous observations [11,12], the as-synthesized g-NCs exhibit an ASE from bulk-like CdS shell, owning to the interfacial potential barrier discussed above.

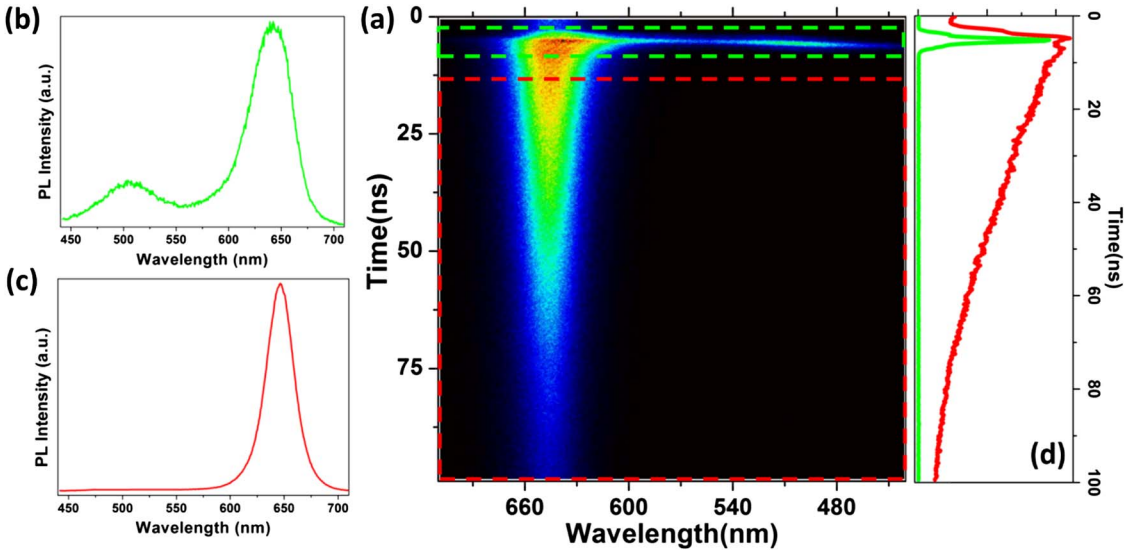

Fig. 3. (a) Streak camera image of time-resolved PL spectra of CdSe/CdS core/shell (15 MLs) g-NCs solution for a laser fluence of 5 mJ/cm^2. PL spectra of the g-NCs as a function of time delay with respect to the laser pulse: (b) delay 0 ns, integrated in a 7 ns gate; (c) delay 11 ns, gate 87 ns. (d) Time-resolved PL decay spectra of the g-NCs measured at 646 nm (red trace) and at 504 nm (green trace).

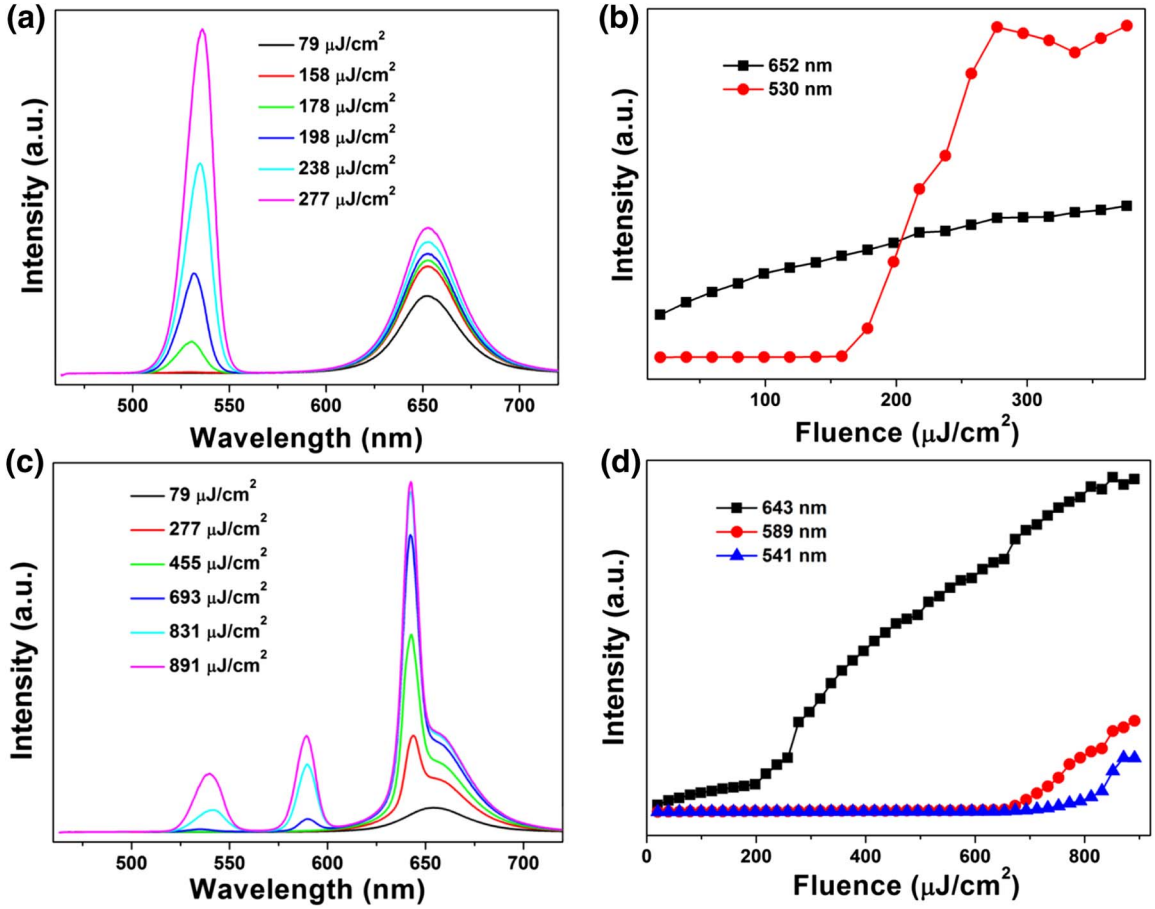

Fig. 4. Emission spectra of a close-packed film of (a) as-synthesized and (c) annealed CdSe/CdS core/shell (15 MLs) g-NCs measured with different per-pulse fluences. Emission intensity versus pump fluence at the positions of ASE and SPE peaks observed for the (b) as-synthesized and (d) annealed g-NCs.

For annealed g-NCs, at low excitation fluences, we only observe SPE at 652 nm. The PL peak of the annealed g-NCs was not blueshifted with respect to that of the as-synthesized g-NCs. In addition, the first-exciton absorption peak does not show any blueshift after annealing, thus indicating that no obvious CdSeS alloy layer is formed in the interface of core and shell. As the fluence increases, a narrower ASE peak at 643 nm corresponding to optical transitions of the first (1S) electron quantization shell of the CdSe core is observed [Fig. 4(c)]. The ASE of the g-NCs shows a typical FWHM of about 9 nm and is blueshifted with respect to the SPE band of the emission band by about 9 nm due to a repulsive character of exciton–exciton interactions in the g-NCs, as discussed above.

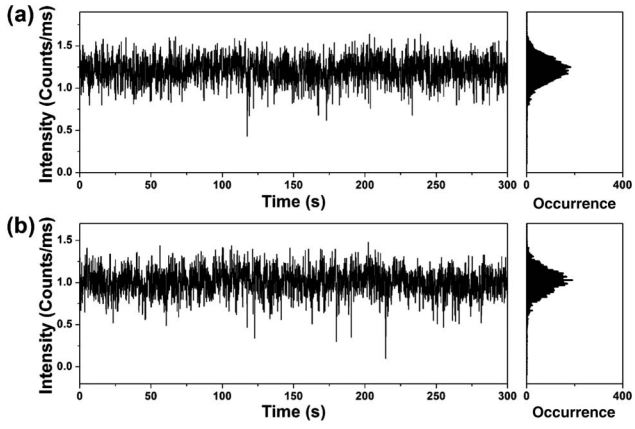

Fig. 5. Time-dependent PL intensity trace of (a) as-synthesized and (b) annealed single CdSe/CdS core/shell (15 MLs) g-NCs (bin size is 100 ms). Histograms indicate the distribution of intensities observed in the trace.

As the pump fluence further increases, besides the ASE at 643 nm, two shorter-wavelength ASE peaks at 589 and 541 nm corresponding to optical transitions of the second (1P) and the third (1D) electron quantization shells of the CdSe core also appear. Within a simple particle in-a-box model [18], the third electron quantized level becomes a population inversion only if the NC contains at least 14 excitons. The core of annealed g-NCs could contain multiexcitons of such a high order because the phase transformation determined with the XRD measurement [Fig. 1(d)] could remove the interfacial barrier. And multiexcitons of such a high order exhibit high emission efficiencies and contribute to optical gain, indicating that Auger recombination is effectively suppressed.

In order to confirm the suppression of Auger recombination, single NC PL measurements were acquired on a confocal microscope. One drop of the diluted solution of g-NCs was spin casted onto a fused silica coverslip to form a solid film. The 480 nm output of a 4.9 MHz, picosecond supercontinuum

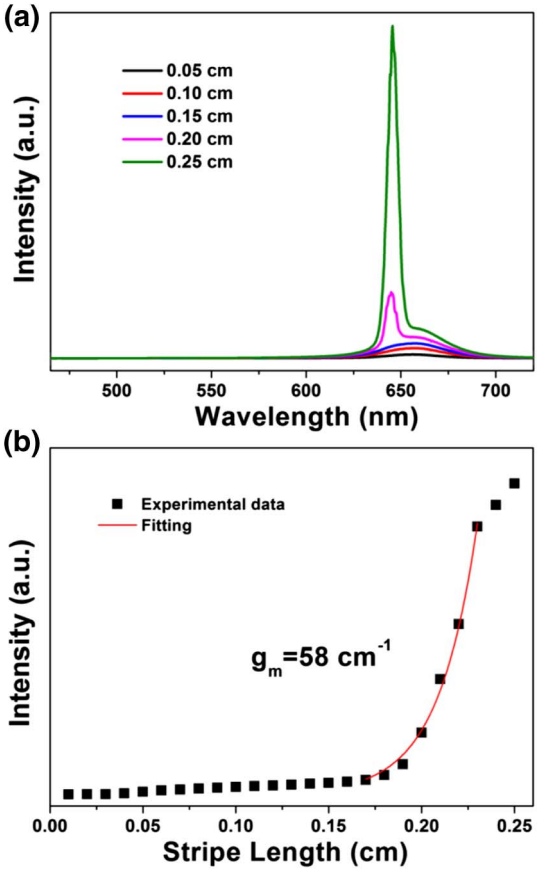

Fig. 6. (a) Emission spectra of a close-packed film of annealed CdSe/CdS core/shell (15 MLs) g-NCs as a function of stripe length obtained from VSL measurement. The pump fluence is 396 μJ/cm^2. (b) Emission intensity versus pump stripe length at the position of ASE peak (643 nm) observed for the annealed g-NCs.

fiber laser (NKT Photonics EXR-15) was used as the excitation source. The laser beam was set at a power density of ~1 W/cm^2 and focused onto the sample substrate by a 100× immersion-oil objective, and the PL signal of a single g-NC collected by the same objective was sent to the avalanche photodiodes in a time-correlated single-photon counting system. The PL intensity trace of as-synthesized and annealed g-NCs (Fig. 5) show long "on" events isolated by occasional short "off" events, confirming that Auger recombination is effectively suppressed.

The thresholds of the three ASE peaks (643, 589, and 541 nm) of the annealed g-NCs film are 208 μJ/cm^2, 623 μJ/cm^2, and 663 μJ/cm^2, respectively. And the modal gain measured by variable stripe length (VSL) method [19] at the first ASE peak (643 nm) is 58 cm^{-1} (Fig. 6). Consider the inherent lower packing density of g-NCs film due to the large size of g-NCs, these results are quite respectable.

The dynamics of optical gain in the annealed g-NCs were studied through a streak camera. The emission decay spectra [Fig. 7(c)] measured at the position of ASE peaks (633, 580, and 525 nm) [Fig. 7(b)] show a pulse-like response with an FWHM of ~10 ps (resolution of the streak camera), thus indicating the ASE of the g-NCs decay faster than 10 ps. The rising edge of the three emission decay spectra show a different delay with respect to the laser pulse, which is due to the dispersion of the measurement system.

4. SUMMARY

In summary, we have demonstrated that the interfacial potential barrier of g-NCs could be removed through laser annealing. As a result, the ASE of the g-NCs transferred from a bulk-like CdS shell to a quantum-confined CdSe core. Besides the ASE at 643 nm, we detect two shorter-wavelength

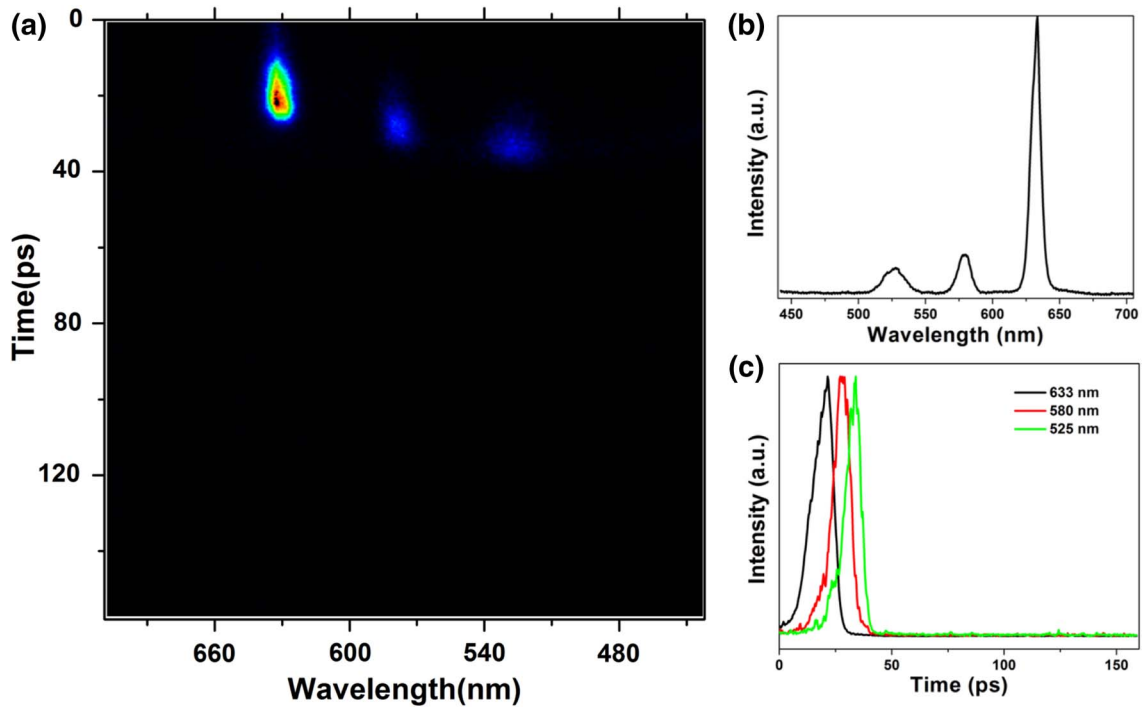

Fig. 7. (a) Streak camera image of time-resolved emission spectra of a close-packed film of annealed CdSe/CdS core/shell (15 MLs) g-NCs for a laser fluence of 891 μJ/cm^2. (b) Emission spectra of the annealed g-NCs (delay 0 ns, integrated in a 50 ps gate). (c) Time-resolved emission decay spectra measured at the position of ASE peaks (633, 580, and 525 nm) observed for the annealed g-NCs.

ASE peaks at 589 and 541 nm corresponding to optical transitions of the second (1P) and the third (1D) electron quantization shells of the CdSe core, indicating that Auger recombination is effectively suppressed. The results highlight that g-NCs have potential applications in producing practical colloidal NCs lasers.

ACKNOWLEDGMENT

This work is supported by the National Basic Research Program of China (973 Program, 2012CB921801), the Science and Technology Department of JiangSu Province (BE2012163), and the Scientific Research Foundation of Graduate School of Southeast University (YBJJ1443).

REFERENCES

1. V. I. Klimov, A. A. Mikhailovsky, S. Xu, A. Malko, J. A. Hollingsworth, C. A. Leatherdale, H.-J. Eisler, and M. G. Bawendi, "Optical gain and stimulated emission in nanocrystal quantum dots," Science **290**, 314–317 (2000).
2. V. I. Klimov, A. A. Mikhailovsky, D. W. McBranch, C. A. Leatherdale, and M. G. Bawendi, "Quantization of multiparticle Auger rates in semiconductor quantum dots," Science **287**, 1011–1013 (2000).
3. Y. Chen, J. Vela, H. Htoon, J. L. Casson, D. J. Werder, D. A. Bussian, V. I. Klimov, and J. A. Hollingsworth, "'Giant' multishell CdSe nanocrystal quantum dots with suppressed blinking," J. Am. Chem. Soc. **130**, 5026–5027 (2008).
4. N. Jagjit, S. A. Ivanov, M. Achermann, I. Bezel, A. Piryatinski, and V. I. Klimov, "Light amplification in the single-exciton regime using exciton-exciton repulsion in type-II nanocrystal quantum dots," J. Phys. Chem. C. **111**, 15382–15390 (2007).
5. F. García-Santamaría, Y. Chen, J. Vela, R. D. Schaller, J. A. Hollingsworth, and V. I. Klimov, "Suppressed Auger recombination in "giant" nanocrystals boosts optical gain performance," Nano Lett. **9**, 3482–3488 (2009).
6. Y.-S. Park, A. V. Malko, J. Vela, Y. Chen, Y. Ghosh, F. García-Santamaría, J. A. Hollingsworth, V. I. Klimov, and H. Htoon, "Near-unity quantum yields of biexciton emission from CdSe/CdS nanocrystals measured using single-particle spectroscopy," Phys. Rev. Lett. **106**, 187401 (2011).
7. Y. Ghosh, B. D. Mangum, J. L. Casson, D. J. Williams, H. Htoon, and J. A. Hollingsworth, "New insights into the complexities of shell growth and the strong influence of particle volume in nonblinking 'giant' core/shell nanocrystal quantum dots," J. Am. Chem. Soc. **134**, 9634–9643 (2012).
8. C. Galland, S. Brovelli, W. K. Bae, L. A. Padilha, F. Meinardi, and V. I. Klimov, "Dynamic hole blockade yields two-color quantum and classical light from dot-in-bulk Nanocrystals," Nano Lett. **13**, 321–328 (2013).
9. S. Brovelli, W. K. Bae, C. Galland, U. Giovanella, F. Meinardi, and V. I. Klimov, "Dual-color electroluminescence from dot-in-bulk nanocrystals," Nano Lett. **14**, 486–494 (2014).
10. S. Brovelli, W. K. Bae, F. Meinardi, B. S. Gonzalez, M. Lorenzon, C. Galland, and V. I. Klimov, "Electrochemical control of two-color emission from colloidal dot-in-bulk nanocrystals," Nano Lett. **14**, 3855–3863 (2014).
11. R. Krahne, M. Zavelani-Rossi, M. G. Lupo, L. Manna, and G. Lanzani, "Amplified spontaneous emission from core and shell transitions in CdSe/CdS nanorods fabricated by seeded growth," Appl. Phys. Lett. **98**, 063105 (2011).
12. Y. Liao, G. Xing, N. Mishra, T. C. Sum, and Y. Chan, "Low threshold, amplified spontaneous emission from core-seeded semiconductor nanotetrapods incorporated into a sol-gel matrix," Adv. Mater. **24**, OP159–OP164 (2012).
13. Y. Liu, C. Zhang, H. Zhang, R. Wang, Z. Hua, X. Wang, J. Zhang, and M. Xiao, "Broadband optical non-linearity induced by charge transfer excitons in type-II CdSe/ZnTe nanocrystals," Adv. Mater. **25**, 4397–4402 (2013).
14. B. Blackman, D. M. Battaglia, T. D. Mishima, M. B. Johnson, and X. Peng, "Control of the morphology of complex semiconductor nanocrystals with a type II heterojunction, dots vs peanuts, by thermal cycling," Chem. Mater. **19**, 3815–3821 (2007).
15. S. J. Lim, B. Chon, T. Joo, and S. K. Shin, "Synthesis and characterization of zinc-blende CdSe-based core/shell nanocrystals and their luminescence in water," J. Phys. Chem. C. **112**, 1744–1747 (2008).
16. X. Peng, M. C. Schlamp, A. V. Kadavanich, and A. P. Alivisatos, "Epitaxial growth of highly luminescent CdSe/CdS core/shell nanocrystals with photostability and electronic accessibility," J. Am. Chem. Soc. **119**, 7019–7029 (1997).
17. F. Meinardi, A. Colombo, K. A. Velizhanin, R. Simonutti, M. Lorenzon, L. Beverina, R. Viswanatha, V. I. Klimov, and S. Brovelli, "Large-area luminescent solar concentrators based on 'Stokes-shift-engineered' nanocrystals in a mass-polymerized PMMA matrix," Nat. Photonics **8**, 392–399 (2014).
18. A. L. Efros and A. L. Efros, "Interband absorption of light in a semiconductor sphere," Sov. Phys. Semicond. **16**, 772–775 (1982).
19. A. V. Malko, A. A. Mikhailovsky, M. A. Petruska, J. A. Hollingsworth, H. Htoon, M. G. Bawendi, and V. I. Klimov, "From amplified spontaneous emission to microring lasing using nanocrystal quantum dot solids," Appl. Phys. Lett. **81**, 1303–1305 (2002).